

# SEISMIC GROUND DEFORMATION MAPPING FOR THE 2017 MW6.1 MAINSHOCK OF SEFIDSANG-NE IRAN EARTHQUAKE USING SENTINEL-1A INTERFEROMETRY



Hamidreza Koohbanani<sup>1</sup>, Sayyed Keivan Hosseini<sup>2</sup>

1 PhD student, Subbatical student, Mashhad, Earthquake Research Center, Ferdowsi university of Mashhad, Iran

2 Assistant Professor, Earthquake Research Center, Ferdowsi university of Mashhad, Iran

**Keywords:** Displacement, InSAR, Sentinel, seismic cycle, Sefidsang

## ABSTRACT

An earthquake of seismic moment magnitude ( $M_w$ )6.1 occurred in northern Iran on April 5th, 2017. In this research, we employed differential interferometric synthetic aperture radar (D-InSAR) technology and Sentinel-1A(S-1A)/IW radar satellite to study the preseismic, coseismic and postseismic deformation of this event. Coseismic surface deformation measurements derived from InSAR analysis revealed a sharp uplifting of ~12 cm resulted from overthrusting and right-lateral strike-slip and the rupture process of the hanging wall in the east southwestward onto the footwall. In this work we discuss about many evidences which support previous hypotheses of motion mechanisms of the Kopeh Dag region in northeastern Iran that has accommodated the deformation due to the collision between Arabia and Eurasia.

## INTRODUCTION

Northeastern Iran is one of the seismically active zones and has suffered a lot of devastating earthquakes over its history, some of which have been accompanied by considerable losses (Berberian and Yeats, 1999). The northeastern Iranian Plateau, which is situated at the eastern most penetration corner of the Arabia-Eurasia plate-collision zone (Jackson, 1992), is experiencing north-south crustal shortening between seismotectonics provinces of Central Iran and Lut Block and the Turan platform. Previous studies have shown that the northward-moving of Arabia with respect to Eurasia is accommodated at a rate of  $22 \pm 2$  mm/a at the longitude of Bahrain (Reilinger et al., 2006) and about 4 to 10 mm/a in northeast of Iran (Shabanian et al., 2009). Most of the north-south convergence has been absorbed by crustal compressing normal to a series of NW–SE-striking mountain ranges, such as the Kuh-E Sorkh, Binalud and Kopeh Dag Mountains (Su et al, 2018).

First, the northward motion of the Lut zone and central Iran with respect to Afghanistan should be taken up between the Doruneh Fault and the Kopeh Dag Mountains with trivial absorption across the northern part of central Iran. Second, part of this motion have to be transferred between the Binalud and Kopeh Dag mountain ranges, as strike-slip motion along localized major fault systems or in form of distributed deformation (on several faults with comparable slip rates).

### InSAR Basics:

Interferometry using InSAR (Interferometric Synthetic Aperture Radar) is the precise method based on the use of at least two SAR images from a special location and is able to discover the changes in vertical displacement accurately at large scale over different time intervals in accuracy of millimetre level (Tang et al., 2016). InSAR has been broadly utilized for surveying the deformation of the earth's surface induced by seismic activities (Amighpey et al, 2009; Feng et al, 2017). The basis of InSAR method is simple. If two SAR images of a region are taken at two different times, the

interferogram for the combination of these two phase images will show slight changes in the Earth's surface on a millimeter scale. SAR imagery is produced by reflecting radar signals off a target area and measuring the two-way travel time back to the satellite (Jeanne et al., 2018). With respect to the Earth's surface in a region that has been scanned twice in a similar geometry, If the radar-Earth-radar distance is the same in both images, the backscatter will be the same, which means that no vertical difference has been made, however, if the surface of the earth crust was affected by some displacements (horizontal or vertical) the radar-Earth-radar distance will be changed and the second image phase will be shifted. This phase shift signifies the displacement of the surface. The amount of motion is corresponding to half the wavelength (Vajedian et al., 2011). So Interferometric Synthetic Aperture Radar (InSAR) is a powerful satellite-based technique for measuring the land deformation (Huang et al., 2017). Our main goal of this work is mapping seismic cycle of Mw6.1 mainshock of Sefidsang 2017 using Sentinel-1A InSAR technique. The Sentinel-1A radar satellite of Europe Space Agency (ESA) was launched on 3 April 2014 designed for interferometric applications to guarantee a very large spatial coverage. The TOPS mode is burst-based, electronically steering the beam periodically in elevation to cover several adjacent sub-swaths.

## Methodology

The Sentinel-1A sensor have been routinely sensing over the plateau of Iran with minimum orbit repeat cycle of 6 days since 2014 at both descending and ascending modes. Specifically, all the accessible descending VV co-polarized C-band images with an interval of 12 days at path 93 and frame 472 have been considered for our research from 2017-03-18 to 2017-05-05. These Single Look Complex (SLC) data, available from ESA data hub in the Interferometric Wide (IW) swath mode, have pixel spacing of about 20m by 5m in azimuth and range components, respectively. The incidence angle of scene center is about 34 degrees. In first step, each interferogram of pair images are calculated individually. The generated interferograms has a phase difference with respect to the initial image and shown in Equation 1.

$$(1) \quad \Delta\phi = \Delta\phi_{orb} + \Delta\phi_{flat} + \Delta\phi_{atm} + \Delta\phi_{noise} + \Delta\phi_{elevation} + \Delta\phi_{displacement} + 2\pi\alpha$$

where,  $\Delta\phi_{orb}$  is the effect of the orbital component,  $\Delta\phi_{flat}$  is the phase difference that caused by the Earth's Spheres,  $\Delta\phi_{atm}$  is the effect of the atmospheric component due to moisture, temperature and air pressure changes in the two acquisition time,  $\Delta\phi_{noise}$  is the phase difference that caused by the temperature of the satellite antennas,  $\Delta\phi_{elevation}$  is the phase difference caused by topography and  $\Delta\phi_{displacement}$  is the phase difference due to the displacement. In fact, the main objective of InSAR is to extract the phase-displacement rate by eliminating or diminishing the effect of other components.  $2\pi\alpha$  is the remainder of the equation that must be removed using the unwrapping method from the final phase. For this step, SNAPHU software was employed to unwrapping final phase. The high coherence of interferograms was mainly achieved by a combination of desert surface and poor vegetation coverage.

## Results and Discussion

Fig. 1 shows the LOS velocity (incidence angle) obtained for the preseismic (No.1), coseismic (No.2) and postseismic (No.3&4) periods, respectively. Positive velocities (blue color) indicate movement toward the satellite.

**Preseismic deformation:** In the preseismic interferogram ("1" in fig 1), some LOS cumulative uplift is recognized on the southern side of the Torbat Jam Fault. This could be hypothetically linked to the accumulated energy before the major earthquake. This trend is reversed in the coseismic interferogram of the mainshock ("2" in fig 1), which may be indicated the sudden release of energy during an earthquake.

**Coseismic deformation:** The detected differences of ground deformation of the co-seismic DInSAR pair could generally be attributed to the cumulative energy release by the aftershock sequence. The surface coseismic displacement showed an upward with a minor left ward slip of

hanging wall in the eastern side of a fault plane with a peak uplifting of ~12 cm along the line-of-sight direction ("2": in fig 1). The seismogenic fault was a thrust fault with minor right-lateral strike-slip shearing. These data indicate that strike-slip faulting also plays a critical role in the slip partitioning of NE Iran.

**Postseismic deformation:** Typically large earthquakes are followed by postseismic displacement in response to coseismic stress changes (Cheng et al., 2009; Gonzalez-Ortega et al., 2014). Differential interferograms (DInSAR) spanning different periods after the main seismic event showed variable ground deformation. For the next 12 days interferogram after mainshock, Fig 1-3 shows a slight uplifting along the Chah-mazar fault (Fig2-4). Spatial proximity of postseismic uplifting of hanging wall indicates the effect of aftershocks on the continuation of fault movements. This postseismic deformation can be attributed to the mainshock. However, the next 12-days interferogram demonstrates the inactivity of the Chah Mazar fault and the reactivity of the Torbat Jam Fault ("4" in fig 1). Undoubtedly in postseismic deformation retrieval, the more data employed, the more comprehensive is the recovered fault slip information.

## Conclusion

One of the most active seismic zones in Iran is Northeastern Iran. The main northern parts of Khorasan-razavi province are geologically located in the Kope Dagh seismotectonics state, but the central parts to the south are located in Binalud and Central Iran states. Accordingly, the earthquake characteristics of this province are affected by evolution of tectonic plates of Kope Dagh, Binalud and Central Iran. The strike-slip faults system in NE Iran play a key role in accommodating the sidelong motion of crust from the convergence front of the Lut Block and Binalud fragments and providing commonly distributed anticlockwise spin around a vertical pivot (Shabanian et al, 2009; Su et al, 2018). Through wide-swath scan data from S-1A/IW, this research derived the preseismic, coseismic and postseismic deformation of the Mw6.1 earthquake that occurred on April 5th, 2017, in Northeastern Iran. Based on Descending path data, we detect an oval-shaped area in 20 km length and 10 km width far about less than 5 km southwest of the epicenter, with largest LOS displacement of 12 cm. Our results show that how the Kopeh Dagh region has been accommodating the deformation due to the collision between Arabia and Eurasia. Also reactivation of this part of Kopeh Dagh should be considered for reassessing the earthquake hazards of this area and shows the importance of geodetic researches beside of seismic studies.

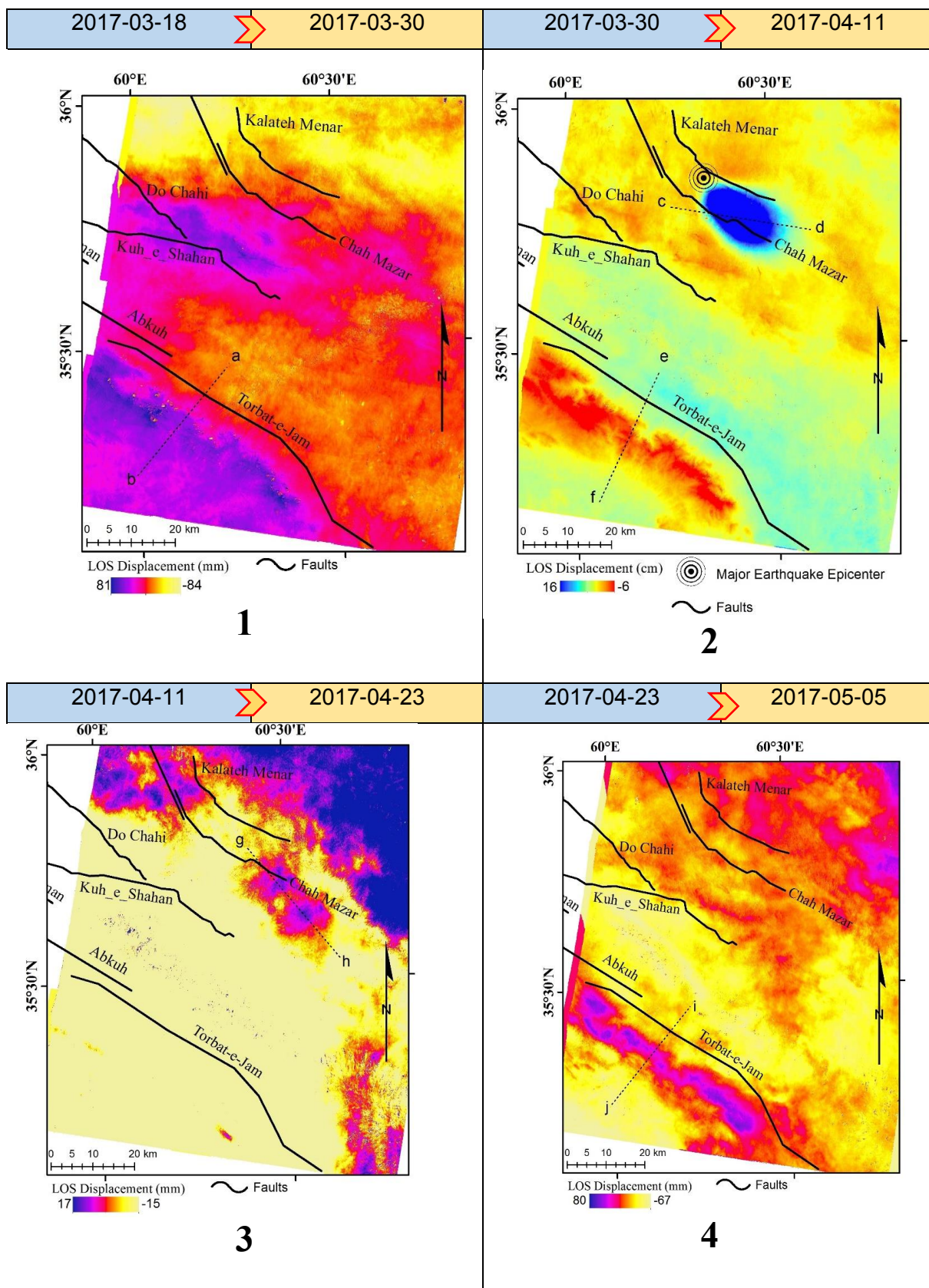


Figure 1. Preseismic (1), Coseismic (2) and postseismic (3,4) deformation velocity obtained from Sentinel-1A InSAR processing

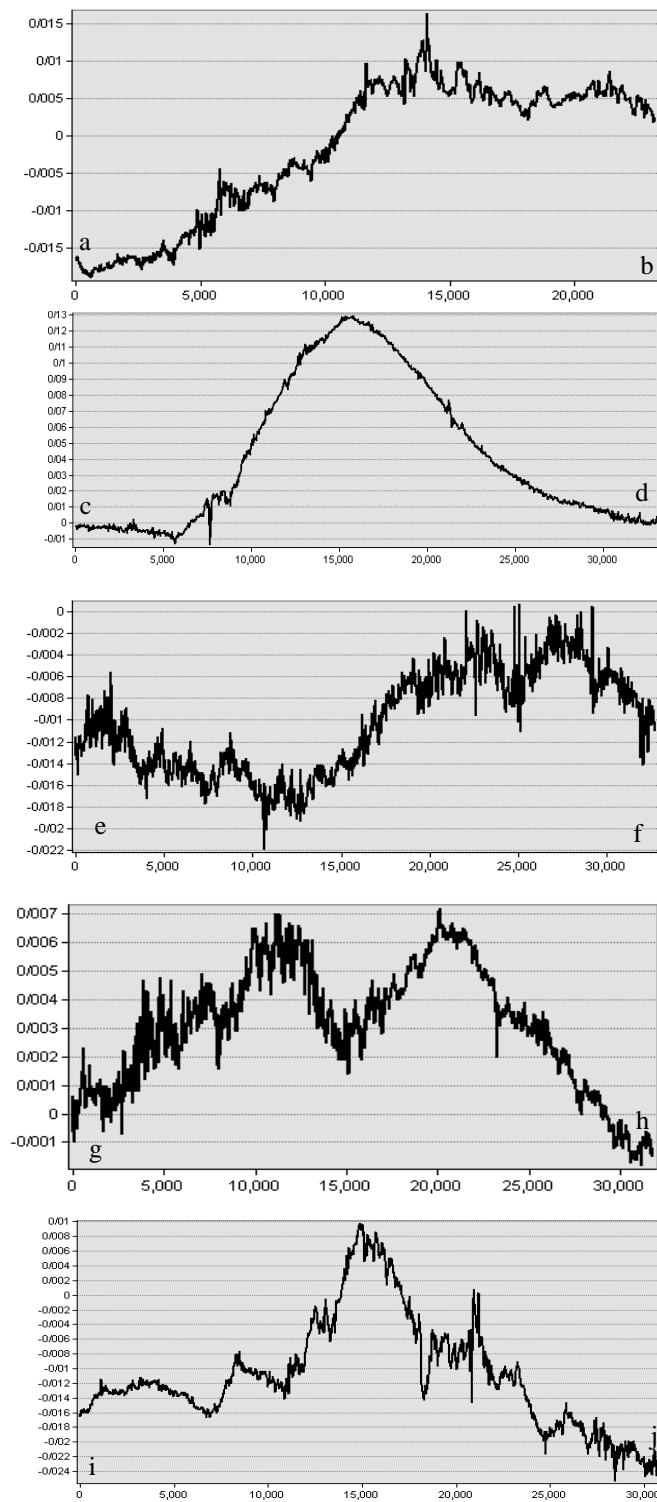


Figure 2. Displacement profiles (The locations of these profiles are shown in Figure 1.)

(X: LOS Displacement (m), Y: Distance (m) )

## REFERENCES

- Amighpey, M., Vosooghi, B., Dehghani, M. (2009). Earth surface deformation analysis of 2005 Qeshm earthquake based on threedimensional displacement field derived from radar imagery measurements. *Applied Earth Observation and Geoinformation* 11: 156-166.
- Berberian, M., Yeats, R. S. (1999). Patterns of historical earthquake rupture in the Iranian Plateau. *Bull. Seismol. Soc. Am.* 89, 120-139.
- Cheng L.W., Lee J.C., Hu J.-C., Chen H.-Y. (2009). Coseismic and postseismic slip distribution of the 2003 Mw = 6.5 Chengkung earthquake in eastern Taiwan: Elastic modeling from inversion of GPS data. *Tectonophysics*. 466(3), 335–343.
- Feng, W., Samsonov, S., Tian, Y., Qiu, Q., Li, P., Zhang, Y., Deng, Z., Omari, K. (2017). Surface deformation associated with the 2015 Mw8.3 Illapel earthquake revealed by satellite-based geodetic observations and its implications for the seismic cycle. *Earth and Planetary Science Letters* 460:222-233.
- Gonzalez-Ortega, A.Y., Fialko, D., Sandwell, F., Nava-Pichardo, A., Fletcher, J., Gonzalez-Garcia, J., Lipovsky, B., Floyd M., Funning G. (2014). El Mayor-Cucapah (Mw 7.2) earthquake: Early near- field postseismic deformation from InSAR and GPS observations. *J. Geophys. Res.*, 119.
- Huang, Q., Crosetto, M., Monserrat, O., Crippa, B. (2017). Displacement monitoring and modelling of a high-speed railway bridge using C-band Sentinel-1 data . *Journal of Photogrammetry and Remote Sensing* 128: 204-211.
- Jackson, J. (1992). Partitioning of strike-slip and convergent motion between eurasia and arabia in eastern turkey and the caucasus. *J. Geophys. Res.: Solid Earth*, 12471-12479.
- Jeanne, P., Farr, T., Rutqvist, J., Vasco, D. (2019). Role of agricultural activity on land subsidence in the San Joaquin Valley, California. *Journal of Hydrology* 569: 462-469.
- Reilinger, R., et al. (2006), GPS constraints on continental deformation in the Africa-Arabia-Eurasia continental collision zone and implications for the dynamics of plate interactions, *J. Geophys. Res.*, 111, B05411, doi:10.1029/2005JB004051.
- Shabanian, E., L. Siame, O. Bellier, L. Benedetti, and M. R. Abbassi. (2009). Quaternary slip rates along the northeast boundary of the Arabia-Eurasia collision zone (Kopeh Dag Mountains, north-east Iran), *Geophys. J. Int.*, 178, 1055 – 1077.
- Su, Z., Yang, y., Li, Y., Xu, X., Zhang, J., Zhou, J., Ren, J., Wang, E., Hu, J., Zhang, S., Talebian, M. (2018). Coseismic displacement of the 5 April 2017 Mashhad earthquake (Mw 6.1) in NE Iran through Sentinel-1A TOPS data: New implications for the strain partitioning in the southern Binalud Mountains, *Asian Earth Sciences* 169: 244-256.
- Tung, H., Chen, H.-Y., Hu, J.-C., Ching, K.-E., Chen, H. and Yang, K.-H. (2016). Transient deformation induced by groundwater change in Taipei metropolitan area revealed by high resolution X-band SAR interferometry. *Tectonophysics* <http://dx.doi.org/10.1016/j.tecto.2016.03.030>.
- Vajediyan, S., Serajiyani, M.R., Mansouri, A. (2010). Extraction of 3D displacement field by using SAR (Case study of Bam Fault), *Journal of Physics of Time and Space*, 37 (2): 83-96.